ISSN 1948-5182 (online)

World Journal of *Hepatology*

World J Hepatol 2024 August 27; 16(8): 1070-1198

Published by Baishideng Publishing Group Inc

World Journal of Hepatology

Contents

Monthly Volume 16 Number 8 August 27, 2024

EDITORIAL

MINIREVIEWS

ORIGINAL ARTICLE

Retrospective Cohort Study

Retrospective Study

Observational Study

Clinical and Translational Research

World Journal of Hepatology

Monthly Volume 16 Number 8 August 27, 2024

Contents

World Journal of Hepatology

Monthly Volume 16 Number 8 August 27, 2024

Contents

ABOUT COVER

Editorial Board Member of *World Journal of Hepatology*, Salvatore Sutti, MSc, PhD, Assistant Professor, Departement of Health Sciences, University of East Piedmont, Novara 28100, Italy. salvatore.sutti@med.uniupo.it

AIMS AND SCOPE

The primary aim of *World Journal of Hepatology* (*WJH*, *World J Hepatol*) is to provide scholars and readers from various fields of hepatology with a platform to publish high-quality basic and clinical research articles and communicate their research findings online.

WJH mainly publishes articles reporting research results and findings obtained in the field of hepatology and covering a wide range of topics including chronic cholestatic liver diseases, cirrhosis and its complications, clinical alcoholic liver disease, drug induced liver disease autoimmune, fatty liver disease, genetic and pediatric liver diseases, hepatocellular carcinoma, hepatic stellate cells and fibrosis, liver immunology, liver regeneration, hepatic surgery, liver transplantation, biliary tract pathophysiology, non-invasive markers of liver fibrosis, viral hepatitis.

INDEXING/ABSTRACTING

The *WJH* is now abstracted and indexed in PubMed, PubMed Central, Emerging Sources Citation Index (ESCI), Scopus, Reference Citation Analysis, China Science and Technology Journal Database, and Superstar Journals Database. The 2024 Edition of Journal Citation Reports® cites the 2023 journal impact factor (JIF) for *WJH* as 2.5; JIF Quartile: Q2. The *WJH*'s CiteScore for 2023 is 4.1 and Scopus CiteScore rank 2023: Hepatology is 41/82.

RESPONSIBLE EDITORS FOR THIS ISSUE

Production Editor: *Yi-Xuan Cai*.; **Production Department Director:** *Xiang Li*; **Cover Editor:** *Xiang Li*.

NAME OF JOURNAL
World Journal of Hepatology

ISSN
ISSN 1948-5182 (online)

LAUNCH DATE
October 31, 2009

FREQUENCY
Monthly

EDITORS-IN-CHIEF
Nikolaos Pyrsopoulos, Ke-Qin Hu, Koo Jeong Kang

EXECUTIVE ASSOCIATE EDITORS-IN-CHIEF
Shuang-Suo Dang

EDITORIAL BOARD MEMBERS
https://www.wjgnet.com/1948-5182/editorialboard.htm

PUBLICATION DATE
August 27, 2024

PUBLISHING PARTNER
Department of Infectious Diseases, the Second Affiliated Hospital of Xi'an Jiaotong University

INSTRUCTIONS TO AUTHORS
https://www.wjgnet.com/bpg/gerinfo/204

GUIDELINES FOR ETHICS DOCUMENTS
https://www.wjgnet.com/bpg/GerInfo/287

GUIDELINES FOR NON-NATIVE SPEAKERS OF ENGLISH
https://www.wjgnet.com/bpg/gerinfo/240

PUBLICATION ETHICS
https://www.wjgnet.com/bpg/GerInfo/288

PUBLICATION MISCONDUCT
https://www.wjgnet.com/bpg/gerinfo/208

POLICY OF CO-AUTHORS
https://www.wjgnet.com/bpg/GerInfo/310

ARTICLE PROCESSING CHARGE
https://www.wjgnet.com/bpg/gerinfo/242

STEPS FOR SUBMITTING MANUSCRIPTS
https://www.wjgnet.com/bpg/GerInfo/239

ONLINE SUBMISSION
https://www.f6publishing.com

PUBLISHING PARTNER's OFFICIAL WEBSITE
http://2yuan.xjtu.edu.cn/Html/Departments/Main/Index_21148.html

World Journal of Hepatology

Submit a Manuscript: https://www.f6publishing.com

World J Hepatol 2024 August 27; 16(8): 1167-1176

DOI: 10.4254/wjh.v16.i8.1167

ISSN 1948-5182 (online)

ORIGINAL ARTICLE

Basic Study

Gadoxetic acid-enhanced magnetic resonance imaging in the assessment of hepatic sinusoidal obstruction syndrome in a mouse model

Yuan-Yuan Chen, Li Yang, Jun Li, Sheng-Xiang Rao, Ying Ding, Meng-Su Zeng

Specialty type: Gastroenterology and hepatology

Provenance and peer review: Unsolicited article; Externally peer reviewed.

Peer-review model: Single blind

Peer-review report's classification

Scientific Quality: Grade C

Novelty: Grade B

Creativity or Innovation: Grade B

Scientific Significance: Grade A

P-Reviewer: Sijens PE

Received: May 15, 2024

Revised: July 13, 2024

Accepted: August 2, 2024

Published online: August 27, 2024

Processing time: 97 Days and 13.9 Hours

Yuan-Yuan Chen, Li Yang, Jun Li, Sheng-Xiang Rao, Ying Ding, Meng-Su Zeng, Department of Radiology, Zhongshan Hospital, Fudan University, Shanghai 200032, China

Corresponding author: Ying Ding, MD, Associate Chief Physician, Department of Radiology, Zhongshan Hospital, Fudan University, No. 180 Fenglin Road, Xuhui District, Shanghai 200032, China. ding.ying@zs-hospital.sh.cn

Abstract

BACKGROUND

Neoadjuvant chemotherapy can cause hepatic sinusoidal obstruction syndrome (SOS) in patients with colorectal cancer liver metastases and increases postoperative morbidity and mortality.

AIM

To evaluate T_1 mapping based on gadoxetic acid-enhanced magnetic resonance imaging (MRI) for diagnosis of hepatic SOS induced by monocrotaline.

METHODS

Twenty-four mice were divided into control (n = 10) and experimental (n = 14) groups. The experimental groups were injected with monocrotaline 2 or 6 days before MRI. MRI parameters were: T1 relaxation time before enhancement; T1 relaxation time 20 minutes after enhancement (T_{1post}); a reduction in T1 relaxation time ($\triangle T_1$%); and first enhancement slope percentage of the liver parenchyma (ESP). Albumin and bilirubin score was determined. Histological results served as a reference. Liver parenchyma samples from the control and experimental groups were analyzed by western blotting, and organic anion transporter polypeptide 1 (OATP1) was measured.

RESULTS

T_{1post}, $\triangle T_1$%, and ESP of the liver parenchyma were significantly different between two groups (all $P < 0.001$) and significantly correlated with the total histological score of hepatic SOS (r = -0.70, 0.68 and 0.79; $P < 0.001$). $\triangle T_1$% and ESP were positively correlated with OATP1 levels (r = 0.82, 0.85; $P < 0.001$), whereas T_{1post} had a negative correlation with OATP1 levels (r = -0.83; $P < 0.001$).

CONCLUSION

T_1 mapping based on gadoxetic acid-enhanced MRI may be useful for diagnosis of hepatic SOS, and MRI parameters were associated with OATP1 levels.

Key Words: T_1 mapping; Gadoxetic acid; Sinusoidal obstruction syndrome; Organic anion transporter polypeptides; Magnetic resonance imaging

Core Tip: Neoadjuvant chemotherapy could cause hepatic sinusoidal obstruction syndrome (SOS) in colorectal liver metastases patients and increases postoperative morbidity and mortality. We used a mouse model of monocrotaline-induced hepatic SOS. We confirmed the relationship between magnetic resonance imaging (MRI) parameters T1 relaxation time 20 minutes after enhancement, a reduction in T1 relaxation time and first enhancement slope percentage of the liver parenchyma and hepatic SOS, suggesting a potential method for the assessment of hepatic SOS. Our results also demonstrated that MRI parameters were correlated with organic anion transporter polypeptide 1 levels.

Citation: Chen YY, Yang L, Li J, Rao SX, Ding Y, Zeng MS. Gadoxetic acid-enhanced magnetic resonance imaging in the assessment of hepatic sinusoidal obstruction syndrome in a mouse model. *World J Hepatol* 2024; 16(8): 1167-1176
URL: https://www.wjgnet.com/1948-5182/full/v16/i8/1167.htm
DOI: https://dx.doi.org/10.4254/wjh.v16.i8.1167

INTRODUCTION

Hepatic sinusoidal obstruction syndrome (SOS) is also known as hepatic veno-occlusive disease of the liver[1]. The main pathological feature of hepatic SOS is damage to liver terminal vessels, and the clinical symptoms of it include ascites and abdominal pain[2]. It was first proposed in 1979 as an early complication of hematopoietic stem cell transplantation[3]. The prevalence ranges from 5% to 60%, and hepatic SOS is a potentially severe complication and can even lead to death in severe cases[4]. Recently, systemic neoadjuvant chemotherapy became widely regarded as one of the causes hepatic SOS in the patients with advanced metastatic colorectal cancer[5,6], especially those were treated with oxaliplatin[7,8].

Oxaliplatin-based preoperative chemotherapy is used for patients with colorectal liver metastases as the standard regimen[8,9], because it could improve tumor resection outcome by shrinking the metastatic sites and reducing recurrence rate[10]. Nevertheless, chemotherapy-induced hepatic SOS has been associated with a higher risk of postresection morbidity[11], such as intraoperative bleeding, intraoperative transfusions, and postoperative liver failure [12]. Therefore, it is important to detect and diagnose of hepatic SOS timely. Currently, the gold standard is still based on liver biopsy[13], but it is an invasive procedure and has several limitations and complications, such as hemorrhage[14]. A noninvasive diagnostic modality is needed for the assessment of hepatic SOS.

Some noninvasive tools have been used for diagnosis of hepatic SOS. Researchers have utilized a preoperative platelet count and aspartate aminotransferase to platelet ratio index[15]. In addition, some imaging methods such as shear wave ultrasonography, computed tomography, and gadoxetic acid-enhanced magnetic resonance imaging (MRI) have been promoted as useful methods for evaluation of hepatic SOS[16-18]. Recent studies with monocrotaline (MCT)-treated rats were conducted to investigate diagnosis and prediction of severity of SOS. For example, intravoxel incoherent motion diffusion-weighted imaging, non-Gaussian diffusion models, and T1 rho quantification[19,20]. The MCT-induced hepatic SOS animal model was reproducible, with a detailed pathological scoring criteria[21].

Gadoxetic acid is a hepatocyte-specific contrast substance, which can provide parenchymal contrast in the hepatobiliary phase. It is reported that gadoxetic acid is absorbed into the liver parenchyma *via* organic anion transporter polypeptide 1 (OATP1) on the hepatocyte membranes[22-24]. Recently, several authors have described the feasibility of gadoxetic acid-enhanced MRI for the diagnosis of oxaliplatin-induced hepatic SOS[25]. They mainly diagnosed hepatic SOS based on the signal intensity of the hepatobiliary specific phase. However, there were several limitations due to the inconsistency between signal intensity of the liver parenchyma and the concentration of contrast agent for evaluation of the degree of hepatic SOS[26]. Therefore, we measured T_1 relaxation time on parametric mapping because it is linearly related to the concentration of the contrast agent and is not affected by other factors[27]. Yang *et al*[28] demonstrated T_1 mapping on gadoxetic acid-enhanced MRI for the assessment of oxaliplatin-induced liver injury in a C57BL/6 mouse model. However, the main pathological changes in their model were hepatocyte degeneration and fibrosis.

Therefore, we aimed to explore the effectiveness of T_1 mapping based on gadoxetic acid-enhanced MRI for the diagnosis of hepatic SOS in a C57BL/6 mouse model, as well as a possible relation between OATP1 Levels and MRI parameters.

MATERIALS AND METHODS

Animal models

Male 6-week-old C57BL/6 mice (17-22 g) were purchased from Shanghai Jiesijie Laboratory Animal Institution (Shanghai, China) and maintained according to the institutional animal care guidelines. Animal experimental procedures were reviewed and approved by our hospital Institutional Ethics and Animal Care. Twenty-four mice were randomly distributed into control (n = 10) and two experimental (n = 7) groups. SOS was induced by MCT as described previously [19]. The experimental mice were injected intraperitoneally (*ip*) with 360 mg/kg MCT, while control mice were treated with tap water. To assess experimental mice with different severity of hepatic SOS, MRI was randomly performed on 2 and 6 days after administration of MCT.

MRI protocols

All examinations were carried out on a 3.0 T MRI scanner (Verio; Siemens Medical Solutions, Erlangen, Germany). During the examination, each mouse was placed in a prone position with a mouse coil and the abdomen of the mouse was restrained with a belt to minimize the effects of respiratory movement: (1) T_1 mapping were obtained before and 20 minutes after the tail vein injection of 0.1 mL/kg gadoxetic acid (Primovist; Bayer Schering Pharma AG, Berlin, Germany), by using a dual flip angle 3D gradient echo sequence with volumetric interpolation breath-holding examination sequence (VIBE): Repetition time (TR), 5.32 millisecond; echo time (TE), 1.73 millisecond; flip angle, 2° and 12°; field of view (FOV), 108 mm; matrix, 160 × 160; slice thickness, 1.5 mm; and R factor, 2; and (2) Dynamic contrast-enhanced (DCE) MRI was performed as the same time as the start of contrast injection, using T1-weighted fast dynamic VIBE: TR, 6.64 millisecond; TE, 1.53 millisecond; flip angle, 9°; FOV, 108 mm; slice thickness, 1.5 mm; R factor, 2; 48 consecutive acquisitions over a period of 6:04 minutes.

Image analysis

All MRI datasets were transmitted to a workstation (Leonardo; Siemens). For T_1 mapping, three regions of interest (ROIs) were chosen at the same locations in the liver parenchyma of the pre- and post-T_1 maps (Figure 1). Each ROI was excluded blood vessels and the margin of liver, and the mean value was taken as the representative of the T_1 relaxation time. All MRIs were measured by a radiologist with 15 years' abdominal imaging experience, who was double-blind to the animal groups and pathology results. The MRI analyses were as follows: (1) Reduction rate of T_1 relaxation time (ΔT_1 %) was quantified as 100% × (T_{1pre} - T_{1post})/T_{1pre}, where T_{1pre} and T_{1post} respectively refers T_1 relaxation time before and after enhancement; and (2) The first rapid enhancement slope percentage (ESP) in the liver parenchyma was quantified as [(SI_{1st} - SI_{base})/SI_{base}] × △T × 100%; where SI_{base} referred to the mean signal value obtained in the first two images after a dynamic enhanced scan; SI_{1st} was the maximum value in the liver parenchyma reached in the first perfusion on the time-signal curve; and △T denoted the interval of time from SI_{base} to SI_{1st}. These data were calculated in custom software on a postprocessing workstation (Mean Curve, Syngo MR B17; Siemens). The same ROIs were selected in the liver parenchyma as those in T_1 mapping. The time-signal curve for the liver parenchyma was also constructed using this software (Figure 2).

Laboratory and histological analysis

After MRI, the mice were anesthetized and humanely killed by cervical dislocation, and blood samples were collected. An upper portion of serum was collected after centrifugation, total bilirubin and albumin levels were determined, and an albumin and bilirubin score (ALBI) was calculated as $\log_{10}$ bilirubin (μmol/L)′ 0.66 + albumin (g/L)′ - 0.085. The liver samples were stained with hematoxylin-eosin (HE) and Masson's dye to examine pathological changes in hepatic structure and to evaluate hepatic SOS. The hepatic SOS histological scores were assessed by a pathologist blinded to the group assignments and imaging results. Histological features of hepatic SOS included sinusoidal hemorrhage, lobular inflammation, endothelial damage to the central vein, subendothelial hemorrhage in the central vein, centrilobular fibrosis, and coagulation necrosis of hepatocytes. Each feature was rated on a four-point scale *via* consensus (0 = absent; 1 = mild; 2 = moderate; and 3 = severe). We calculated the final pathology score by summing the individual scores of the six features.

OATP1 detection

Western blotting was performed to quantify OATP levels: (1) Protein extraction: The liver specimen was washed with ice-cold phosphate buffer three times, and an appropriate amount of lysis buffer was supplemented with benzyl sulfonyl fluoride to a final concentration of 1 mmol/L. Lysis buffer (100 μL) was added per 10 mg tissue; the mixture was shaken for 2 minutes in a 4-gauge homogenizer until full disintegration; and the supernatant was collected after 5 minutes of centrifugation at 10000 *g*; (2) Protein quantification: A human BCA working solution was prepared by mixing reagents A and B of the BCA Protein Quantitative Kit (Beyotime, Shanghai) at a volume ratio of 50:1. An appropriate amount of each liver tissue sample was placed into a 1.5 mL centrifuge tube; isosmotic saline was added to obtain a total volume of 100 μL; and 1 mL human BCA working solution was added. The protein concentration was calculated from the standard curve; (3) PAGE: This assay was carried out on a Bole electrophoresis apparatus (Bio-Rad, Hercules, CA, United States). The protein samples (lysates) were electrophoresed until the dye reached the top of the separation gel at a constant voltage of 120 V, and when bromophenol blue was just out of the loading gel, they were electrophoresed at a constant voltage of 160 V; and (4) Immunoassay: After a fresh sealing solution was prepared, skimmed milk powder was added to Tris-buffered saline supplemented with 0.05% of Tween 20 (TBST) to a final concentration of 0.05 kg/L. A diluted primary antibody was incubated with the samples overnight at 4 °C. The type and concentration of the antibody were as follows: A rabbit anti-mouse OATP1 antibody and the dilution ratio of 1:1000.

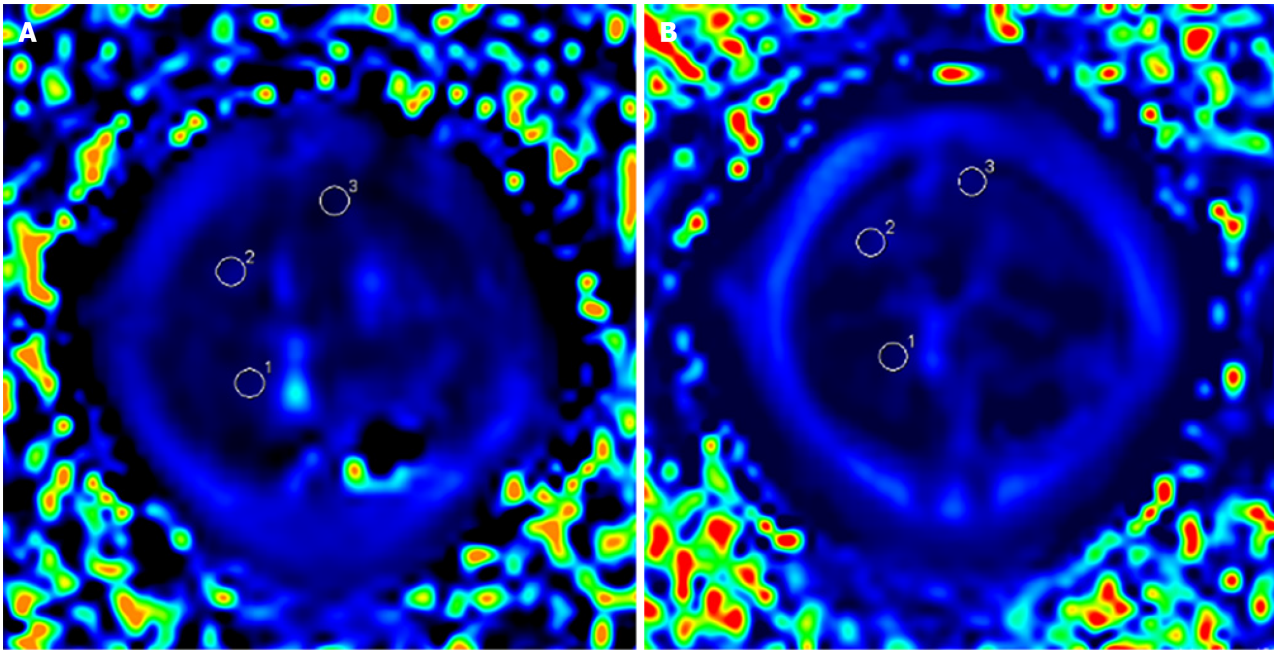

Figure 1 Regions of interest in the same area in the liver parenchyma before and after enhancement in the same C57BL/6 mouse. A: Before enhancement in the same C57BL/6 mouse; B: After enhancement in the same C57BL/6 mouse. [1]The region of interest in the middle hepatic lobe are delineated to avoid blood vessels within the liver parenchyma; [2]The region of interest in the right hepatic lobe are delineated to avoid blood vessels within the liver parenchyma; [3] The region of interest in the right hepatic lobe are delineated to avoid blood vessels within the liver parenchyma.

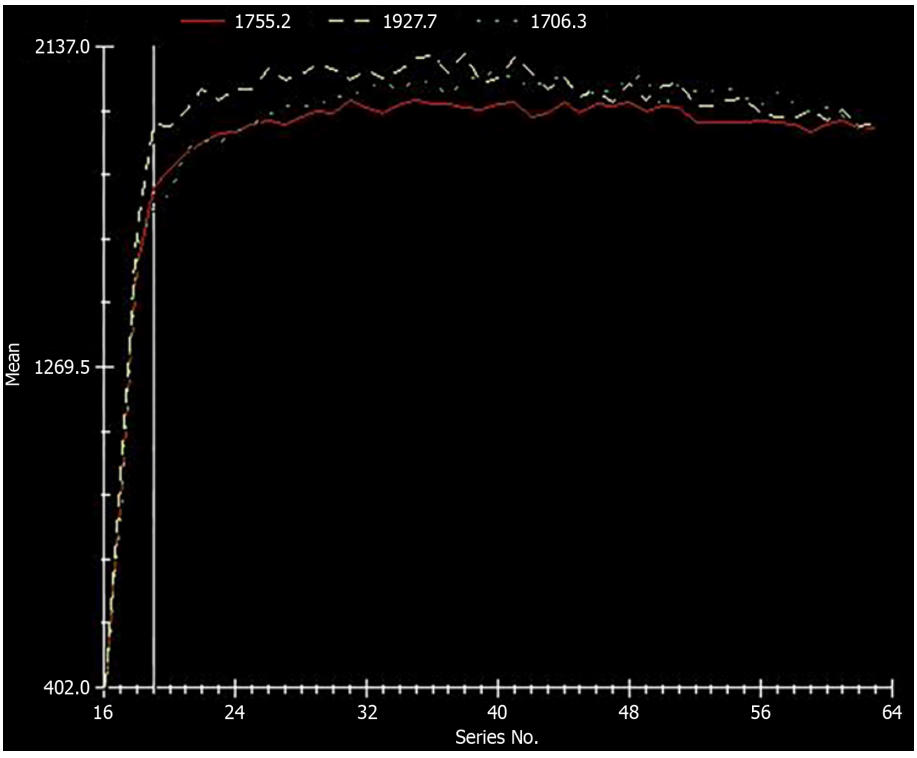

Figure 2 Liver parenchyma time–signal curve: The x axis represents the time axis, and the y axis represents T1 relaxation time, and the slope represents the first rapid enhancement slope percentage. The three lines represent the values of the three regions of interest (ROIs). We selected the same ROIs in the liver parenchyma for T_1 mapping.

Statistical analysis

Descriptive statistics were calculated for MRI parameters, ALBI and OATP1 levels, and were presented as mean ± SD. Statistical significance was performed by using the student's *t* test between groups. Spearman's rank correlation coefficient was calculated to evaluate the correlation between histological scores and individual MRI parameters, ALBI. The correlation between individual MRI parameters, ALBI and OATP1 Levels was assessed using Pearson's correlation. *P*

< 0.05 was considered statistically significant. All data analyses were performed SPSS 26 (IBM Corp., Armonk, NY, United States).

RESULTS

Animal models

One mouse died during the experiment period; therefore, there were 13 mice in the experimental group. In the HE and Masson staining findings, sinusoidal hemorrhage and endothelial damage to the central vein were noted in each mouse in the experimental group, whereas there was no endothelial damage in the control group. Table 1 summarizes the results of the histopathological examination. Typical samples from the experimental groups are shown in Figure 3. Table 2 presents the correlations between MRI parameters and the total histological scores. T_{1pre} showed no correlation with the total histological score (r = 0.37, P = 0.095), T_{1post} had a negative correlation with the total histological score of hepatic SOS (r = -0.70, P < 0.001), whereas ΔT_1% and ESP (r = 0.68, 0.79, P < 0.001) significantly increased with the total histological of hepatic SOS. ALBI was also decreased with the total histological of hepatic SOS (r = -0.76, P < 0.001).

Comparisons of MRI parameters and ALBI between the control and experimental groups

Table 3 and Figure 4 show the comparisons of MRI parameters and ALBI between the control and experimental groups. Among the MRI parameters, T_{1pre} showed no significant difference between the control and experimental groups, whereas T_{1post}, ΔT_1%, and ESP did. The SOS-mice had a significantly lower T_{1post} than the normal mice had (P < 0.001), and the difference in mean T_{1post} between the control and experimental groups was 288 milliseconds; ΔT_1% and ESP were significantly higher in the SOS than in the control group (P < 0.001, P < 0.001), and the difference between the groups was 46.56% and 15.53%, respectively. ALBI also significantly differed between the control and experimental groups.

OATP1 Levels between the control and experimental groups

The levels of OATP1 in the control and experimental groups were 29952 ± 11475 and 422060 ± 178634, which was a significant difference (P < 0.001).

Correlations of MRI parameters, ALBI and OATP1 levels

In Pearson's correlation analysis, T_{1pre} showed no correlation with OATP1 (r = 0.06, P = 0.457). ΔT_1% and ESP were strongly positively correlated with OATP1 levels (r = 0.82, 0.85, respectively; P < 0.001), whereas T_{1post} was negatively correlated with OATP1 levels (r = -0.83; P < 0.001; Table 4). In addition, ALBI exhibited a moderate negative correlation with OATP1 Levels (r = -0.56; P = 0.005).

DISCUSSION

In this study, we used a mouse model of MTC-induced hepatic SOS. We confirmed the relationship between MRI parameters T_{1post}, △T1% and ESP and hepatic SOS, suggesting a potential method for the assessment of hepatic SOS. Our results also demonstrated that MRI parameters were correlated with OATP1 levels.

We showed that T_{1post} and $\triangle T_1$% had significant differences between the control and experimental groups and were associated with total histological score. Several previous studies[29,30] have reported that T_1 mapping on gadoxetic acid-enhanced MRI could reflect the liver function in rats with hepatic fibrosis and found that T_{1post} and $\triangle T_1$% could be better than apparent diffusion coefficient for assessing the rate of liver necro-inflammatory activity and stage of liver fibrosis. Yang *et al*[28] showed that T1 relaxation time and $\triangle T_1$% might be a sensitive tool for diagnosis of oxaliplatin-induced liver injury by using gadoxetic acid-enhanced MRI. However, they did not explore the relationship between OATP1 Levels and MRI parameters. After injection, gadoxetic acid is gradually taken into the liver parenchyma through OATP1 on the hepatocyte membranes. Our experimental group also found that T_{1post} and $\triangle T_1$% were correlated with expression of OATP1, which was consistent with the literature. Previous studies[31,32] have confirmed that OATP1a1 measurement had a negative correlation with gadoxetic acid in liver fibrosis rats caused by carbon tetrachloride. A recent case[32] reported a patient with hepatic SOS, indicating that changes in expression of OATP seem to be related to the appearance of a low signal in the hepatobiliary phase. These results indicate that T_{1post} and $\triangle T_1$% are reliable methods for diagnosis of hepatic SOS. Gadoxetic acid-enhanced MRI could be applied clinically to examine hepatic SOS in colorectal cancer patients treated with oxaliplatin prior to liver surgery.

In addition to T_{1post} and $\triangle T_1$%, our findings suggested that ESP was helpful for the evaluation of hepatic SOS. ESP exhibited a significant difference between the experimental and control mice. Both animal and human studies have demonstrated the potential of perfusion parameters acquired from DCE-MRI with gadoxetic acid in the assessment of liver function and fibrosis[33,34]. However, the analysis of hepatic DCE-MRI involves complex mathematical modeling, and no model has been generally accepted at present[35]. We calculated ESP to evaluate hemodynamic changes in the liver, which could be easily adapted to clinical practice. Previous research found that ESP of the liver could assess bile duct ligation caused by cholestatic liver injury and has diagnostic efficacy[36]. Our data showed that the ESP was significantly higher in SOS than in the control liver. These findings were consistent with several previous research[36,37]. Chen *et al*[37] found that arterial fraction was elevated with the severity of liver fibrosis by using DCE-MRI with gadoxetic acid-enhanced MRI in patients with chronic hepatitis. Wu *et al*[38] also showed that the fraction of hepatic

Table 1 Histological features in sinusoidal obstruction syndrome

No.	Central vein endothelial damage	Central vein subendothelial hemorrhage	Sinusoidal hemorrhage	Lobular inflammation	Hepatocyte necrosis	Centrilobular fibrosis	All scores
1	2	1	2	1	0	0	6
2	0	1	1	0	0	0	2
3	1	1	1	1	0	0	4
4	1	1	1	0	0	0	3
5	0	1	1	0	0	2	2
6	1	0	0	1	0	0	2
7	1	0	0	0	0	0	1
8	1	1	0	1	1	1	5
9	1	1	1	1	0	1	5
10	2	2	1	1	1	1	8
11	1	2	1	1	0	1	6
12	1	2	2	1	1	1	8
13	2	3	3	3	0	0	11

Each pathological feature was assessed using a 4-point grading system: 0 = absent; 1 = mild; 2 = moderate; 3 = severe. All score = total scores of the six pathological features.

Table 2 Correlations between magnetic resonance imaging, albumin bilirubin, and total histological score

	T_{1pre}	T_{1post}	$\triangle T_1\%$	ESP	ALBI
r	0.37	-0.70	0.68	0.79	-0.76
P value	0.095	< 0.001	< 0.001	< 0.001	< 0.001

T_{1pre}: T1 relaxation time before enhancement; T1post: T1 relaxation time 20 minutes after enhancement; △T1%: Reduction rate of T1 relaxation time; ESP: The first enhancement slope percentage in liver parenchyma; ALBI: Albumin and bilirubin.

Table 3 Magnetic resonance imaging and albumin/bilirubin in control and experimental groups

Parameters	Control group (*n* = 10)	Experimental group (*n* = 13)	*P* value
T_{1pre} (millisecond)	659.13 ± 24.07	681.57 ± 40.58	0.137
T_{1post} (millisecond)	408.87 ± 27.21	120.48 ± 53.71	< 0.001
$\triangle T_1\%$	37.84 ± 5.46	82.40 ± 7.62	< 0.001
ESP	4.14 ± 0.95	19.67 ± 12.12	< 0.001
ALBI	0.95 ± 0.04	0.12 ± 0.89	< 0.001

T_{1pre}: T1 relaxation time before enhancement; T_{1post}: T1 relaxation time 20 minutes after enhancement; $\triangle T_1\%$: Reduction rate of T1 relaxation time; ESP: The first enhancement slope percentage in liver parenchyma; ALBI: Albumin and bilirubin.

arterial blood volume increased with severity of nonalcoholic fatty liver disease or in fibrotic liver. Based on the results of our study and previous literature, we hypothesized that hepatic SOS might increase blood flow in the damaged liver. Nevertheless, further studies are required to explain this phenomenon.

ALBI grade is a newly proposed, simple, and significant tool for assessment of liver function[39]. Our data revealed the ALBI scores of SOS were significantly different from the ALBI score of the normal liver. A recent study showed mathematical combinations with ALBI were able to identify chemotherapy-associated liver injury[40], which supports that ALBI might be a noninvasive tool for detecting hepatic SOS. Nevertheless, ALBI reflected the whole-liver function, while

Table 4 Correlation between magnetic resonance imaging, albumin/bilirubin and organic transporter polypeptide 1

	r	*P* value
T_{1pre}	-0.06	0.803
T_{1post}	-0.83	< 0.001
$\triangle T_1$%	0.82	< 0.001
ESP	0.85	< 0.001
ALBI	-0.56	0.005

T_{1pre}: T1 relaxation time before enhancement; T_{1post}: T1 relaxation time 20 min after enhancement; $\triangle T_1$%: Reduction rate of T1 relaxation time; ESP: The first enhancement slope percentage in liver parenchyma; ALBI: Albumin and bilirubin; OATP1: Organic transporter polypeptide 1.

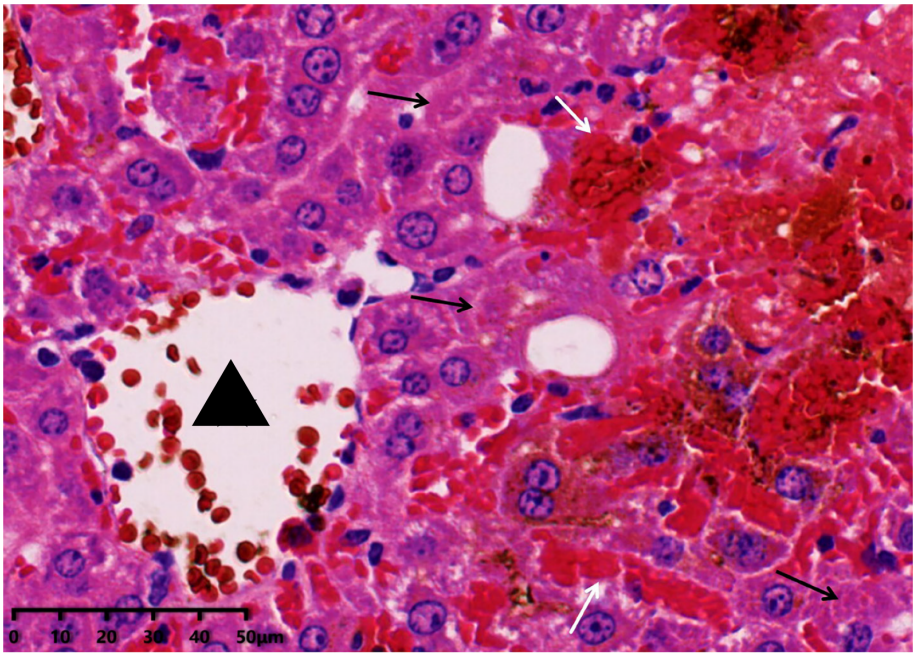

Figure 3 Hematoxylin and eosin staining (400 ×). Histological findings of monocrotaline mouse models, the liver specimen demonstrates sinusoidal hemorrhage and hepatocytes necrosis, which are characteristic findings of sinusoidal obstruction syndrome. The triangle represents the central vein, the white arrow indicates dilated hepatic sinusoids hemorrhage, and the black arrow indicates hepatocyte necrosis.

gadoxetic acid-enhanced MRI could provide information of regional liver function. Zhou *et al*[41] indicated that T_1 mapping based on gadoxetic acid-enhanced MRI could be used to assess the function of hepatic segments. This suggested that gadoxetic acid-enhanced MRI could better reflect liver function than laboratory examination index.

There are other imaging techniques that have been suggested to be helpful for detecting hepatic SOS. For example, Park *et al*[42] confirmed the potential of acoustic-radiation-pulsed elastography for diagnosis, severity evaluation and follow-up of hepatic SOS in animal models. However, the application of ultrasound elastography has limitations and the results rely more on the subjective judgment of the examiners. Hong *et al*[19] and Lyu *et al*[20] respectively demonstrated the traditional double-exponential Gaussian model and non-Gaussian model to diagnose the severity of hepatic SOS. Compared with other tools, gadoxetic acid-enhanced MRI also can detect chemotherapy-related focal nodular hyperplasia-like lesions and accurately identify liver metastases, and it can allow "one-stop shopping" in one examination.

There were some limitations to our research. First, our study involved MCT-induced SOS, which was considered as a reproducible animal model, rather than clinical oxaliplatin-induced SOS. Second, the sample size was small; however, T_{1post} and $\triangle T_1$% were significantly associated with the severity of hepatic SOS. A large sample size study on humans should be researched to confirm these results.

CONCLUSION

In conclusion, our findings suggest that T_1 mapping on gadoxetic acid-enhanced MRI was suitable for detecting hepatic SOS. In addition, we conclude that T_1 relaxation time correlated with OATP1.

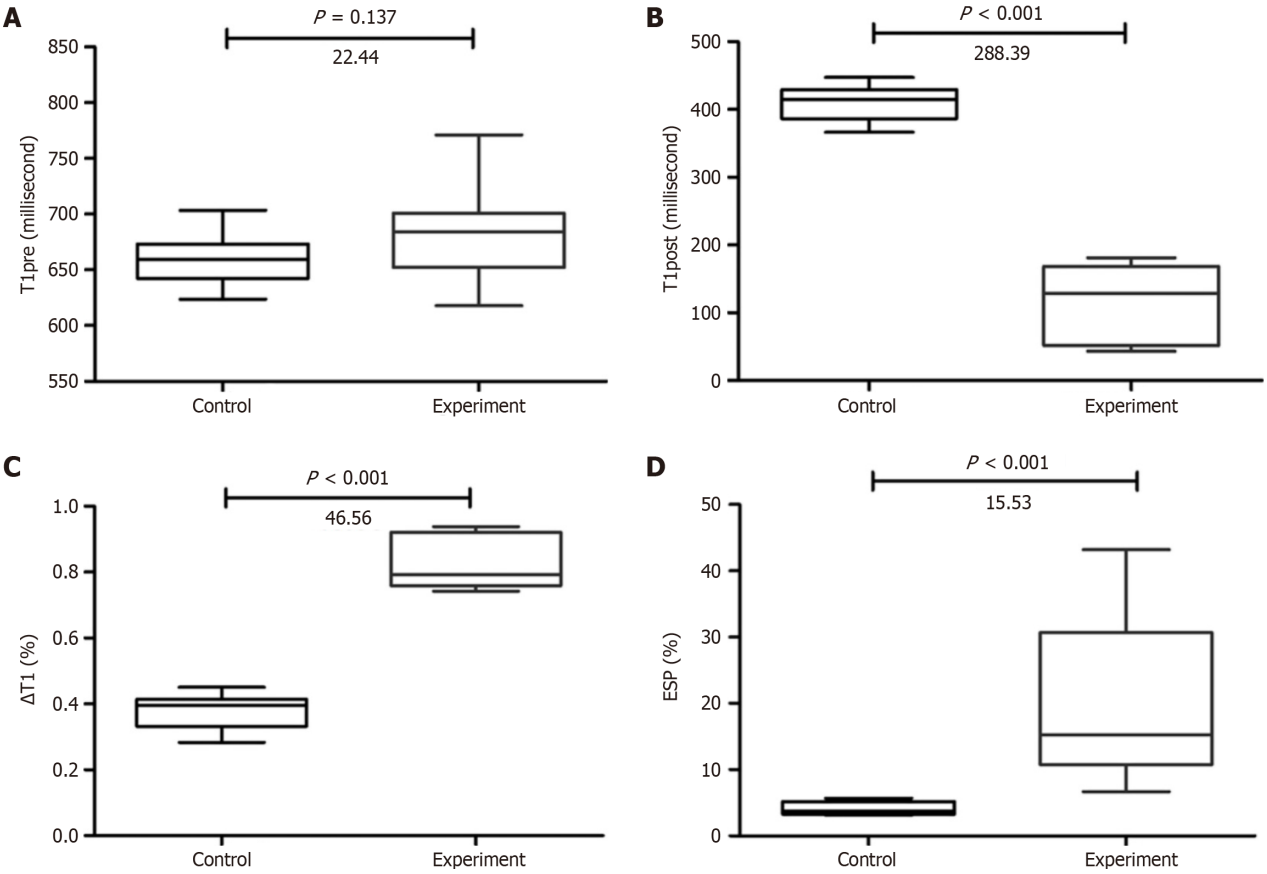

Figure 4 Box plots in control and experimental groups. A: Box plots of T1 relaxation time before enhancement (T1pre); B: T1 relaxation times 20 minutes after enhancement (T1post); C: The reduction of T1 relaxation time (△T1%); D: The first enhancement slope percentage of the liver parenchyma in control and experimental groups. T_{1pre}: T1 relaxation time before enhancement; T1post: T1 relaxation time 20 minutes after enhancement; △T1%: Reduction rate of T1 relaxation time; ESP: The first enhancement slope percentage in liver parenchyma.

FOOTNOTES

Author contributions: Chen YY contributed to the conception, design, acquisition, analysis, interpretation of data, wrote the manuscript; Yang L and Li J collected and preprocessed the data; Rao SX provided supervision and methodology; Ding Y revised the manuscript and gave the final approval of the version to be published; Zeng MS was responsible for conceptualization and supervision.

Supported by the National Science Foundation for Young Scientists of China, No. 81701682.

Institutional animal care and use committee statement: Animal experimental procedures were reviewed and approved by Zhongshan Hospital Institutional Ethics and Animal Care on February 4, 2017.

Conflict-of-interest statement: All the authors report no relevant conflicts of interest for this article.

Data sharing statement: The data that support the findings of this study are available from the corresponding author upon reasonable request at ding.ying@zs-hospital.sh.cn.

ARRIVE guidelines statement: The authors have read the ARRIVE Guidelines, and the manuscript was prepared and revised according to the ARRIVE Guidelines.

Country of origin: China

ORCID number: Yuan-Yuan Chen 0000-0003-2342-145X; Sheng-Xiang Rao 0000-0001-7722-8327; Ying Ding 0000-0002-4478-3436.

S-Editor: Li L
L-Editor: A

P-Editor: Zhang L

REFERENCES

1 **Valla DC**, Cazals-Hatem D. Sinusoidal obstruction syndrome. *Clin Res Hepatol Gastroenterol* 2016; **40**: 378-385 [PMID: 27038846 DOI: 10.1016/j.clinre.2016.01.006]

2 **Rubbia-Brandt L**. Sinusoidal obstruction syndrome. *Clin Liver Dis* 2010; **14**: 651-668 [PMID: 21055688 DOI: 10.1016/j.cld.2010.07.009]

3 **Jacobs P**, Miller JL, Uys CJ, Dietrich BE. Fatal veno-occlusive disease of the liver after chemotherapy, whole-body irradiation and bone marrow transplantation for refractory acute leukaemia. *S Afr Med J* 1979; **55**: 5-10 [PMID: 371033]

4 **Mohty M**, Malard F, Abecassis M, Aerts E, Alaskar AS, Aljurf M, Arat M, Bader P, Baron F, Bazarbachi A, Blaise D, Ciceri F, Corbacioglu S, Dalle JH, Duarte RF, Fukuda T, Huynh A, Masszi T, Michallet M, Nagler A, NiChonghaile M, Pagluica T, Peters C, Petersen FB, Richardson PG, Ruutu T, Savani BN, Wallhult E, Yakoub-Agha I, Carreras E. Sinusoidal obstruction syndrome/veno-occlusive disease: current situation and perspectives-a position statement from the European Society for Blood and Marrow Transplantation (EBMT). *Bone Marrow Transplant* 2015; **50**: 781-789 [PMID: 25798682 DOI: 10.1038/bmt.2015.52]

5 **Han NY**, Park BJ, Sung DJ, Kim MJ, Cho SB, Lee CH, Jang YJ, Kim SY, Kim DS, Um SH, Won NH, Yang KS. Chemotherapy-induced focal hepatopathy in patients with gastrointestinal malignancy: gadoxetic acid--enhanced and diffusion-weighted MR imaging with clinical-pathologic correlation. *Radiology* 2014; **271**: 416-425 [PMID: 24475862 DOI: 10.1148/radiol.13131810]

6 **Zhao J**, van Mierlo KMC, Gómez-Ramírez J, Kim H, Pilgrim CHC, Pessaux P, Rensen SS, van der Stok EP, Schaap FG, Soubrane O, Takamoto T, Viganò L, Winkens B, Dejong CHC, Olde Damink SWM; Chemotherapy-Associated Liver Injury (CALI) consortium. Systematic review of the influence of chemotherapy-associated liver injury on outcome after partial hepatectomy for colorectal liver metastases. *Br J Surg* 2017; **104**: 990-1002 [PMID: 28542731 DOI: 10.1002/bjs.10572]

7 **Rubbia-Brandt L**, Audard V, Sartoretti P, Roth AD, Brezault C, Le Charpentier M, Dousset B, Morel P, Soubrane O, Chaussade S, Mentha G, Terris B. Severe hepatic sinusoidal obstruction associated with oxaliplatin-based chemotherapy in patients with metastatic colorectal cancer. *Ann Oncol* 2004; **15**: 460-466 [PMID: 14998849 DOI: 10.1093/annonc/mdh095]

8 **Zorzi D**, Laurent A, Pawlik TM, Lauwers GY, Vauthey JN, Abdalla EK. Chemotherapy-associated hepatotoxicity and surgery for colorectal liver metastases. *Br J Surg* 2007; **94**: 274-286 [PMID: 17315288 DOI: 10.1002/bjs.5719]

9 **Macedo FI**, Makarawo T. Colorectal hepatic metastasis: Evolving therapies. *World J Hepatol* 2014; **6**: 453-463 [PMID: 25067997 DOI: 10.4254/wjh.v6.i7.453]

10 **Bismuth H**, Adam R. Reduction of nonresectable liver metastasis from colorectal cancer after oxaliplatin chemotherapy. *Semin Oncol* 1998; **25**: 40-46 [PMID: 9609107]

11 **Nakano H**, Oussoultzoglou E, Rosso E, Casnedi S, Chenard-Neu MP, Dufour P, Bachellier P, Jaeck D. Sinusoidal injury increases morbidity after major hepatectomy in patients with colorectal liver metastases receiving preoperative chemotherapy. *Ann Surg* 2008; **247**: 118-124 [PMID: 18156931 DOI: 10.1097/SLA.0b013e31815774de]

12 **Aloia T**, Sebagh M, Plasse M, Karam V, Lévi F, Giacchetti S, Azoulay D, Bismuth H, Castaing D, Adam R. Liver histology and surgical outcomes after preoperative chemotherapy with fluorouracil plus oxaliplatin in colorectal cancer liver metastases. *J Clin Oncol* 2006; **24**: 4983-4990 [PMID: 17075116 DOI: 10.1200/JCO.2006.05.8156]

13 **Castera L**. Invasive and non-invasive methods for the assessment of fibrosis and disease progression in chronic liver disease. *Best Pract Res Clin Gastroenterol* 2011; **25**: 291-303 [PMID: 21497746 DOI: 10.1016/j.bpg.2011.02.003]

14 **Piccinino F**, Sagnelli E, Pasquale G, Giusti G. Complications following percutaneous liver biopsy. A multicentre retrospective study on 68,276 biopsies. *J Hepatol* 1986; **2**: 165-173 [PMID: 3958472 DOI: 10.1016/s0168-8278(86)80075-7]

15 **Soubrane O**, Brouquet A, Zalinski S, Terris B, Brézault C, Mallet V, Goldwasser F, Scatton O. Predicting high grade lesions of sinusoidal obstruction syndrome related to oxaliplatin-based chemotherapy for colorectal liver metastases: correlation with post-hepatectomy outcome. *Ann Surg* 2010; **251**: 454-460 [PMID: 20160638 DOI: 10.1097/SLA.0b013e3181c79403]

16 **Oki E**, Kakeji Y, Taketomi A, Yamashita Y, Ohgaki K, Harada N, Iguchi T, Shibahara K, Sadanaga N, Morita M, Maehara Y. Transient elastography for the prediction of oxaliplatin-associated liver injury in colon cancer patients: a preliminary analysis. *J Gastrointest Cancer* 2008; **39**: 82-85 [PMID: 19377909 DOI: 10.1007/s12029-009-9063-1]

17 **Han NY**, Park BJ, Kim MJ, Sung DJ, Cho SB. Hepatic Parenchymal Heterogeneity on Contrast-enhanced CT Scans Following Oxaliplatin-based Chemotherapy: Natural History and Association with Clinical Evidence of Sinusoidal Obstruction Syndrome. *Radiology* 2015; **276**: 766-774 [PMID: 25822471 DOI: 10.1148/radiol.2015141749]

18 **Ünal E**, Karaosmanoğlu AD, Ozmen MN, Akata D, Karcaaltincaba M. Hepatobiliary phase liver MR imaging findings after Oxaliplatin-based chemotherapy in cancer patients. *Abdom Radiol (NY)* 2018; **43**: 2321-2328 [PMID: 29427046 DOI: 10.1007/s00261-018-1482-7]

19 **Hong EK**, Joo I, Park J, Lee K. Assessment of hepatic sinusoidal obstruction syndrome with intravoxel incoherent motion diffusion-weighted imaging: An experimental study in a rat model. *J Magn Reson Imaging* 2020; **51**: 81-89 [PMID: 31094055 DOI: 10.1002/jmri.26790]

20 **Lyu J**, Yang G, Mei Y, Guo L, Guo Y, Zhang X, Xu Y, Feng Y. Non-Gaussian Diffusion Models and T(1) rho Quantification in the Assessment of Hepatic Sinusoidal Obstruction Syndrome in Rats. *J Magn Reson Imaging* 2020; **52**: 1110-1121 [PMID: 32246796 DOI: 10.1002/jmri.27156]

21 **DeLeve LD**, Valla DC, Garcia-Tsao G; American Association for the Study Liver Diseases. Vascular disorders of the liver. *Hepatology* 2009; **49**: 1729-1764 [PMID: 19399912 DOI: 10.1002/hep.22772]

22 **Joo I**, Lee JM. Recent Advances in the Imaging Diagnosis of Hepatocellular Carcinoma: Value of Gadoxetic Acid-Enhanced MRI. *Liver Cancer* 2016; **5**: 67-87 [PMID: 26989660 DOI: 10.1159/000367750]

23 **Van Beers BE**, Pastor CM, Hussain HK. Primovist, Eovist: what to expect? *J Hepatol* 2012; **57**: 421-429 [PMID: 22504332 DOI: 10.1016/j.jhep.2012.01.031]

24 **Kudo M**. Will Gd-EOB-MRI change the diagnostic algorithm in hepatocellular carcinoma? *Oncology* 2010; **78** Suppl 1: 87-93 [PMID: 20616589 DOI: 10.1159/000315235]

25 **Shin NY**, Kim MJ, Lim JS, Park MS, Chung YE, Choi JY, Kim KW, Park YN. Accuracy of gadoxetic acid-enhanced magnetic resonance imaging for the diagnosis of sinusoidal obstruction syndrome in patients with chemotherapy-treated colorectal liver metastases. *Eur Radiol*

2012; **22**: 864-871 [PMID: 22108766 DOI: 10.1007/s00330-011-2333-x]

26 **Bae KE**, Kim SY, Lee SS, Kim KW, Won HJ, Shin YM, Kim PN, Lee MG. Assessment of hepatic function with Gd-EOB-DTPA-enhanced hepatic MRI. *Dig Dis* 2012; **30**: 617-622 [PMID: 23258104 DOI: 10.1159/000343092]

27 **Kamimura K**, Fukukura Y, Yoneyama T, Takumi K, Tateyama A, Umanodan A, Shindo T, Kumagae Y, Ueno S, Koriyama C, Nakajo M. Quantitative evaluation of liver function with T1 relaxation time index on Gd-EOB-DTPA-enhanced MRI: comparison with signal intensity-based indices. *J Magn Reson Imaging* 2014; **40**: 884-889 [PMID: 24677659 DOI: 10.1002/jmri.24443]

28 **Yang L**, Ding Y, Rao S, Chen C, Zeng M. T(1) Mapping on Gd-EOB-DTPA-Enhanced MRI for the Prediction of Oxaliplatin-Induced Liver Injury in a Mouse Model. *J Magn Reson Imaging* 2021; **53**: 896-902 [PMID: 32979019 DOI: 10.1002/jmri.27377]

29 **Ding Y**, Rao SX, Zhu T, Chen CZ, Li RC, Zeng MS. Liver fibrosis staging using T1 mapping on gadoxetic acid-enhanced MRI compared with DW imaging. *Clin Radiol* 2015; **70**: 1096-1103 [PMID: 26164421 DOI: 10.1016/j.crad.2015.04.014]

30 **Giraudeau C**, Leporq B, Doblas S, Lagadec M, Pastor CM, Daire JL, Van Beers BE. Gadoxetate-enhanced MR imaging and compartmental modelling to assess hepatocyte bidirectional transport function in rats with advanced liver fibrosis. *Eur Radiol* 2017; **27**: 1804-1811 [PMID: 27553933 DOI: 10.1007/s00330-016-4536-7]

31 **Sheng RF**, Wang HQ, Yang L, Jin KP, Xie YH, Fu CX, Zeng MS. Assessment of liver fibrosis using T1 mapping on Gd-EOB-DTPA-enhanced magnetic resonance. *Dig Liver Dis* 2017; **49**: 789-795 [PMID: 28237298 DOI: 10.1016/j.dld.2017.02.006]

32 **Yoneda N**, Matsui O, Ikeno H, Inoue D, Yoshida K, Kitao A, Kozaka K, Kobayashi S, Gabata T, Ikeda H, Nakamura K, Ohta T. Correlation between Gd-EOB-DTPA-enhanced MR imaging findings and OATP1B3 expression in chemotherapy-associated sinusoidal obstruction syndrome. *Abdom Imaging* 2015; **40**: 3099-3103 [PMID: 26187715 DOI: 10.1007/s00261-015-0503-z]

33 **Lagadec M**, Doblas S, Giraudeau C, Ronot M, Lambert SA, Fasseu M, Paradis V, Moreau R, Pastor CM, Vilgrain V, Daire JL, Van Beers BE. Advanced fibrosis: Correlation between pharmacokinetic parameters at dynamic gadoxetate-enhanced MR imaging and hepatocyte organic anion transporter expression in rat liver. *Radiology* 2015; **274**: 379-386 [PMID: 25289480 DOI: 10.1148/radiol.14140313]

34 **Dyvorne HA**, Jajamovich GH, Bane O, Fiel MI, Chou H, Schiano TD, Dieterich D, Babb JS, Friedman SL, Taouli B. Prospective comparison of magnetic resonance imaging to transient elastography and serum markers for liver fibrosis detection. *Liver Int* 2016; **36**: 659-666 [PMID: 26744140 DOI: 10.1111/liv.13058]

35 **Liao YS**, Lee LW, Yang PH, Kuo LM, Kuan LY, Tseng WI, Hwang DW. Assessment of liver cirrhosis for patients with Child's A classification before hepatectomy using dynamic contrast-enhanced MRI. *Clin Radiol* 2019; **74**: 407.e11-407.e17 [PMID: 30799098 DOI: 10.1016/j.crad.2019.01.017]

36 **Ding Y**, Rao SX, Chen C, Li R, Zeng MS. Potential of Gd-EOB-DTPA-enhanced MR imaging for evaluation of bile duct ligation-induced liver injury in rabbits. *Hepatol Int* 2015; **9**: 303-309 [PMID: 25788184 DOI: 10.1007/s12072-014-9595-8]

37 **Chen BB**, Hsu CY, Yu CW, Wei SY, Kao JH, Lee HS, Shih TT. Dynamic contrast-enhanced magnetic resonance imaging with Gd-EOB-DTPA for the evaluation of liver fibrosis in chronic hepatitis patients. *Eur Radiol* 2012; **22**: 171-180 [PMID: 21879400 DOI: 10.1007/s00330-011-2249-5]

38 **Wu Z**, Cheng ZL, Yi ZL, Xie MW, Zeng H, Lu LJ, Xu X, Shen J. Assessment of Nonalcoholic Fatty Liver Disease in Rats Using Quantitative Dynamic Contrast-Enhanced MRI. *J Magn Reson Imaging* 2017; **45**: 1485-1493 [PMID: 27606822 DOI: 10.1002/jmri.25455]

39 **Hiraoka A**, Kumada T, Michitaka K, Kudo M. Newly Proposed ALBI Grade and ALBI-T Score as Tools for Assessment of Hepatic Function and Prognosis in Hepatocellular Carcinoma Patients. *Liver Cancer* 2019; **8**: 312-325 [PMID: 31768342 DOI: 10.1159/000494844]

40 **Pereyra D**, Rumpf B, Ammann M, Perrodin SF, Tamandl D, Haselmann C, Stift J, Brostjan C, Laengle F, Beldi G, Gruenberger T, Starlinger P. The Combination of APRI and ALBI Facilitates Preoperative Risk Stratification for Patients Undergoing Liver Surgery After Neoadjuvant Chemotherapy. *Ann Surg Oncol* 2019; **26**: 791-799 [PMID: 30617869 DOI: 10.1245/s10434-018-07125-6]

41 **Zhou ZP**, Long LL, Qiu WJ, Cheng G, Huang LJ, Yang TF, Huang ZK. Evaluating segmental liver function using T1 mapping on Gd-EOB-DTPA-enhanced MRI with a 3.0 Tesla. *BMC Med Imaging* 2017; **17**: 20 [PMID: 28249571 DOI: 10.1186/s12880-017-0192-x]

42 **Park SH**, Lee SS, Sung JY, Na K, Kim HJ, Kim SY, Park BJ, Byun JH. Noninvasive assessment of hepatic sinusoidal obstructive syndrome using acoustic radiation force impulse elastography imaging: A proof-of-concept study in rat models. *Eur Radiol* 2018; **28**: 2096-2106 [PMID: 29218616 DOI: 10.1007/s00330-017-5179-z]

Published by **Baishideng Publishing Group Inc**
7041 Koll Center Parkway, Suite 160, Pleasanton, CA 94566, USA
Telephone: +1-925-3991568
E-mail: office@baishideng.com
Help Desk: https://www.f6publishing.com/helpdesk
https://www.wjgnet.com